International Journal of Biological Macromolecules 174 (2021) 32–41

Contents lists available at ScienceDirect

International Journal of Biological Macromolecules

journal homepage: http://www.elsevier.com/locate/ijbiomac

Urea titration of a lipase from *Pseudomonas* sp. reveals four different conformational states, with a stable partially folded state explaining its high aggregation propensity

Minoo Qafary [a,b], Khosro Khajeh [c], Matteo Ramazzotti [b], Ali Akbar Moosavi-Movahedi [a,*], Fabrizio Chiti [b,**]

[a] Institute of Biochemistry and Biophysics, University of Tehran, Tehran, Iran
[b] Department of Biomedical, Experimental and Clinical Sciences, Section of Biochemistry, University of Florence, Viale Morgagni 50, 50134 Florence, Italy
[c] Department of Biochemistry, Faculty of Biological Sciences, Tarbiat Modares University, Tehran, Iran

ARTICLE INFO

Article history:
Received 29 August 2020
Received in revised form 14 January 2021
Accepted 22 January 2021
Available online 27 January 2021

Keywords:
Lipase
Fibrillation
Protein misfolding
Neurodegenerative disease
Fibrillation mechanism

ABSTRACT

The conversion of soluble proteins into amyloid fibrils has importance in protein chemistry, biology, biotechnology and medicine. A novel lipase from *Pseudomonas* sp. was previously shown to have an extremely high aggregation propensity. It was therefore herein studied to elucidate the physicochemical and structural determinants of this extreme behaviour. Amyloid-like structures were found to form in samples up to 2.5–3.0 M using Thioflavin T fluorescence and Congo red binding assays. However, dynamic light scattering (DLS), static light scattering and turbidimetry revealed the existence of aggregates up to 4.0 M urea, without amyloid-like structure. Two monomeric conformational states were detected with intrinsic fluorescence, 8-anilinonaphthalene-1-sulfonate (ANS) binding and circular dichroism. These were further characterized in 7.5 M and 4.5 M urea using enzymatic activity measurements, tryptophan fluorescence quenching, DLS and nuclear magnetic resonance (NMR) and were found to consist of a largely disordered and a partially folded state, respectively, with the latter appearing stable, cooperative, fairly compact, non-active, α-helical, with largely buried hydrophobic residues. The persistence of a stable structure up to high concentrations of urea, in the absence of sequence characteristics typical of a high intrinsic aggregation propensity, explains the high tendency of this enzyme to form amyloid-like structures.

1. Introduction

Biological fluids of any living organism — be they Eubacteria, Archaea, lower eukaryotes or mammals — are colloidal aqueous solutions where different, highly concentrated proteins can potentially aggregate into large deleterious assemblies. The resulting assemblies often consist of well-organized fibrillar assemblies held together by continuous β-sheet structures running along the fibril axis, generally referred to as amyloid fibrils [1,2]. From a purely physicochemical perspective, the conversion of proteins from their native state into amyloid fibrils is an essential property of protein behaviour [1,2]. Elucidation of this behaviour is vital for a thorough characterization of the nature of proteins — for example to decipher their folding code and how protein sequences have evolved [2]. Protein aggregation is also a major issue in biotechnology, because the large-scale production of peptides and proteins of industrial or pharmaceutical interest often results in their aggregation [3]. From a reversed biotechnological viewpoint, amyloid fibril formation by peptides and proteins can also turn out to be useful, as a large number of novel materials can be designed by exploiting the amyloid motif [4]. In biology, protein aggregation is a constant challenge for any living organism and to this purpose all of them have evolved dedicated systems to prevent it, collectively known as protein homeostasis [5,6]. In fact, failure of proteins and peptides to remain soluble may result into pathology and indeed a number of human diseases are associated with the formation of fibrillar aggregates, including the most common forms of neurodegeneration [1,7].

Given the importance of the process of amyloid fibril formation to protein chemistry, biotechnology, biology and medicine, it is very important to elucidate the mechanisms by which proteins convert from their soluble states into amyloid fibrils. In this context, a novel lipase from a *Pseudomonas* sp. isolated in Southern Iran (taxonomy identifier 114,707) is an interesting and clear-cut system, because it was shown to aggregate into amyloid fibrils very rapidly and under a wide range

Abbreviations: IBs, inclusion bodies; ThT, thioflavin T; CR, congo red; D_h, apparent hydrodynamic diameter; DLS, dynamic light scattering; CD, circular dichroism; ANS, 8-anilinonaphthalene-1-sulfonic acid; NMR, nuclear magnetic resonance; LB, Luria Broth; IPTG, isopropyl-β-D-1-thiogalactopyranoside; DTT, dithiothreitol; Kcps, kilocounts per second.

* Corresponding author.
** Correspondence to: F. Chiti, Viale Morgagni 50, I-50134 Florence, Italy.
E-mail addresses: moosavi@ut.ac.ir (A.A. Moosavi-Movahedi), fabrizio.chiti@unifi.it (F. Chiti).

https://doi.org/10.1016/j.ijbiomac.2021.01.153
0141-8130/

of experimental conditions, including conditions of pH and temperature close to physiological [8–10]. In particular, a ten-fold dilution of the protein initially solubilized and denatured in 8.0 M urea resulted in the rapid formation, on the time-scale of a few seconds, of assemblies positive for thioflavin T (ThT) and Congo red (CR) and containing extensive β-sheet structure, followed by the appearance of amyloid fibrils in a few hours, as observed with transmission electron microscopy [8,9]. This was found under a variety of experimental conditions optimized to slow down aggregation and to promote its solubility and folding [9]. In fact, the protein is generally purified in a denatured state following a resolubilization procedure from inclusion bodies (IBs) at high urea concentrations and requires its lipase specific foldase, coded by the gene immediately downstream of the lipase gene, to refold [11,12]. Lipases are also enzymes that constitute an important group of biocatalysts for biotechnological applications [13]. In fact, this group of enzymes catalyze the hydrolysis of long chain triglycerides [14] and is applied as a biocatalyst in food, agriculture, pharmaceutical, chemical, cosmetic, flavor, detergent and agriculture products [14–17].

In this work we have studied the structural properties of this lipase enzyme under different urea concentrations at pH 8.0 and 25 °C and using a number of spectroscopic probes, in the search of the structural properties of the non-native urea-unfolded state that make this protein a unique case in terms of its dramatically high aggregation propensity. Urea titration was used as a means of establishing gradients of destabilizing conditions for native, partially folded and aggregated lipase, so that different conformational states could be observed as urea concentration increases. We will show that following urea titration the protein forms four distinct conformational states under the conditions of pH, temperature, protein concentration and time explored here, including β-sheet containing aggregates, α-helical containing aggregates, a stable monomeric partially folded state enriched with α-helical structure and a largely unstructured state, with the progressive increase of denaturant concentration. The α-helical partially folded state, either aggregated or monomeric, was found to be populated up to 5.5 M urea and to be remarkably stable, contributing to explain the high propensity of this lipase protein to aggregate and why it requires its specific foldase to refold.

2. Materials and methods

2.1. Lipase expression and purification

A single colony of previously transformed *E. coli* BL21 cells with the pET-28a vector containing the gene coding for lipase from *Pseudomonas* sp. were cultured in 10 ml Luria Broth (LB) medium containing 50 μg/ml kanamycin under vigorous shaking overnight at 37 °C. Next, 1 l of liquid LB was inoculated with a 1% sample of precultured bacteria in the same condition. After reaching the OD_{600} value of 0.6–0.8, protein expression was induced with 1 mM isopropyl-β-D-1-thiogalactopyranoside (IPTG). Following 6 h of induction at 30 °C, cells and culture medium were separated by centrifugation at 3700*g* for 10 min. Cells in the pellet were suspended in 20 ml lysis buffer containing 50 mM Tris-HCl, 500 mM NaCl, pH 8.0.

After the disruption of cells with sonication in ice (6 cycles of 10 s burst with a frequency of 90 Hz followed by a 30 s interval of cooling), IBs were collected with centrifugation at 12,500*g* for 20 min at 4 °C. IBs were dissolved in 20 ml of 50 mM Tris-HCl buffer, pH 8.0, containing 8.0 M urea and 1 mM dithiothreitol (DTT) and were then incubated at 25 °C for at least 1 h. After equilibrating a Nickel Agarose column with 50 mM Tris-HCl, pH 8.0, containing 8.0 M urea and 300 mM NaCl, 25 °C, the solubilized IBs were loaded onto the column. The unbound proteins were washed with 50 mM Tris-HCl, pH 8.0, containing 8.0 M urea and 30 mM imidazole. The pure protein was eluted with the same buffer containing 300 mM imidazole. SDS-PAGE was applied for checking the purity of the eluted fractions. Pure lipase fractions were pooled and concentrated using Amicon Ultra-15 centrifugal filter devices with 10,000 molecular-weight cut-off and 15 ml capacity. Lipase concentration was determined spectrophotometrically using an ε_{280} value of 27,515 M^{-1} cm^{-1}. The purified protein contained 317 residues, including the 28-residue signal peptide and the 6-residue His-Tag at the N- and C-terminus, respectively. It was maintained at −20 °C.

2.2. Sample preparation

The protein stock contained 16 mg/ml lipase in 50 mM Tris-HCl, 8.0 M urea, pH 8.0. It was filtered using a 0.02 μm filter just before preparing the samples. The 16 mg/ml lipase sample was diluted to reach a final concentration of 2.0 mg/ml (60 μM) of lipase and urea concentrations ranging from 1.0 to 8.0 M with 0.5 M steps. The samples were incubated at 25 °C for 24 h before starting the assays. For Thioflavin T assay, turbidimetry and dynamic light scattering, lipase concentration was 1.0 mg/ml (30 μM) and for NMR, lipase concentration was 3.3 mg/ml (100 μM).

2.3. Thioflavin T (ThT) assay

ThT was dissolved to 25 μM in 50 mM Tris-HCl buffer, pH 8.0, at different concentrations of urea ranging from 1.0 to 8.0 M and the resulting solutions were filtered through a 0.45 μm syringe filter. The 25 μM ThT solutions were adjusted spectrophotometrically using an ε_{412} value of 36,000 M^{-1} cm^{-1}. 10 μL of lipase sample at a given urea concentration were added to 290 μL of ThT solution containing the same urea concentration. ThT fluorescence spectra were recorded using the excitation wavelength of 440 nm and an emission range of 475–600 nm, by a BioTek Synergy H1 plate reader (Winooski, VT, USA) at 25 °C and averaged over three scans. The excitation and emission slits were 3 nm and 6 nm, respectively. ThT fluorescence spectra were also measured in corresponding conditions in the absence of protein as blanks.

2.4. Congo red (CR) binding assay

CR was dissolved fresh to 20 μM in 5 mM phosphate buffer, 150 mM NaCl, pH 7.4, at different concentrations of urea ranging from 1.0 to 8.0 M and the resulting solutions were filtered through a 0.45 μm syringe filter. 30 μL of lipase sample at a given urea concentration were mixed with 220 μL of 20 μM CR solution containing the same urea concentration. A BioTek Synergy H1 plate reader (Winooski, VT, USA) was used to acquire the absorption spectra of CR with or without protein and of protein without CR at 25 °C in the 400–700 nm wavelength range. For the whole range of urea concentration, the difference absorbance value at 540 nm (ΔAbsorbance) was calculated using the following equation:

$$\Delta\text{Absorbance} = A - B - C \quad (1)$$

where A, B and C are the absorbance values of CR with protein, CR without protein and protein without CR, respectively, all at 540 nm and all blank-subtracted.

2.5. Dynamic light scattering (DLS)

The DLS measurements were carried out on lipase samples using a Malvern Panalytical Zetasizer Nano S instrument (Malvern, Worcestershire, UK) and using disposable polystyrene cuvettes with a 1-cm path length. For all solutions, the appropriate viscosity and refractive index values were set according to their urea concentrations. The cells position and attenuator were fixed at 4.65 and 9.0, respectively. All measurements were carried out three times and the average distributions were reported.

2.6. Turbidimetry

The turbidity measurements were carried out on lipase samples at 600 nm using a Jasco V-630 spectrophotometer (Tokyo, Japan) and a 5 mm path-length quartz cell. All values were blank subtracted.

2.7. Intrinsic fluorescence

The intrinsic fluorescence spectra of the various lipase samples were recorded using a 2 × 10-mm path length cuvette and a PerkinElmer LS 55 fluorimeter (Waltham, MA, USA) equipped with a thermostated cell compartment attached to a Haake F8 water bath (Karlsruhe, Germany) at 25 °C. The excitation wavelength was 280 nm and the emission range was recorded from 295 to 495 nm. The excitation and emission slits were 3 nm and 6 nm, respectively. All spectra were acquired 3 times and the average distributions were reported.

2.8. 8-Anilinonaphthalene-1-sulfonic acid (ANS) assay

Solutions of 50 μM ANS in 50 mM Tris-HCl buffer, pH 8.0, containing different concentrations of urea from 1.0 to 8.0 M were prepared and the resulting solutions were filtered with 0.22 μm cut-off filters. The concentrations of the 50 μM ANS solutions were adjusted by UV-absorbance using an ε_{375} value of 8000 M^{-1} cm^{-1}. For all urea concentrations, 75 μL of lipase sample at a given urea concentration was mixed with 925 μL of 50 μM ANS solution containing the same concentration of urea. The fluorescence spectra were recorded using an excitation wavelength of 380 nm and an emission range of 400 to 600 nm by an Agilent Cary Eclipse fluorescence spectrophotometer (Agilent Technologies, Santa Clara, CA, USA) and using a 4 × 10-mm path length cuvette and averaged over three scans. The excitation and emission slits were 5 nm and 10 nm, respectively. The spectra were also recorded for all the corresponding ANS solutions in the absence of protein as blanks.

2.9. Circular dichroism (CD) spectroscop

Far-UV CD spectra of lipase samples were recorded by a Jasco J-810 spectropolarimeter (Tokyo, Japan) equipped with a thermostated cell holder attached to a Haake C25P water bath (Karlsruhe, Germany) and a 1.0-mm path length cuvette. The spectra were recorded at 25 °C from 190 to 260 nm and averaged over three scans. All spectra were blank-subtracted, normalized to mean residue ellipticity and truncated when the HT signal was above 700 V.

2.10. Enzymatic activity measurements

Lipase was refolded in 0.0 M urea in the presence of its specific foldase, as previously reported [18]. The enzymatic activity of refolded lipase was measured in 0.0 M urea (folded state) and non-refolded lipase in 2.0, 3.5, 4.5 and 7.5 M urea at 25 °C using *p*-Nitrophenyl palmitate (pNPP) as substrate, as previously reported [12]. In brief, the enzymatic cocktail was prepared by adding 3 mg of pNPP to 1 ml of 2-propanol and then to 9 ml of 50 mM Tris-HCl buffer, pH 8.0, containing 0.4% (*w*/*v*) Triton X-100 and 0.1% (w/v) Arabic gum. Aliquots of lipase samples (20 μl) were mixed with 180 μl of the enzymatic reactions and were incubated at 37 °C for 5 min. The hydrolysis of pNPP was monitored by optical absorption at 410 nm by a BioTek Synergy H1 plate reader (Winooski, VT, USA).

2.11. Fluorescence quenching by acrylamide

Two samples containing 0.5 mg/ml of lipase in 4.5 M and 7.5 M urea, respectively, were prepared. Intrinsic fluorescence spectra were measured using a BioTek Synergy H1 plate reader (Winooski, VT, USA) in the absence of acrylamide and in the presence of progressive additions of small volumes of 2.5 M acrylamide to final concentrations of 0–125 mM. The emission spectra were acquired using an excitation wavelength of 280 nm and an emission range of 320–450 nm, were blank subtracted and then corrected to account for the dilution caused by the addition of the acrylamide solution aliquots. The data were analyzed using a procedure of best fitting and the following equation:

$$(F_0/F) = 1 + K_{SV}\,[Q] \quad (2)$$

where F_0 and F are the recorded total fluorescence intensities in the absence and presence of quencher (acrylamide) in the wavelength range 320–450 nm, [Q] is the molar concentration of the quencher and K_{SV} is the Stern-Volmer constant, free to float in the fitting procedure.

2.12. Nuclear magnetic resonance (NMR)

An *E. coli* strain containing the lipase construct was grown in M9 minimal media by using ^{15}N-enriched NH_4Cl. The lipase labelled with ^{1}H and ^{15}N was expressed and purified as described above. The purified lipase in 8.0 M urea, 50 mM Tris-HCl, pH 8.0, was then buffer-exchanged using 8.0 M urea-d4 in D_20. The samples containing 4.5 M and 7.5 M urea-d4 with final protein concentration of 3.3 mg/ml (100 μM) were prepared as described above. The 1D ^{1}H NMR and 2D ^{15}N-^{1}H-HSQC NMR spectra were acquired on a Bruker Avance 700 MHz NMR spectrometer at 25 °C using a 3 mm NMR tube. Typically, a sweep width of 12 and 35 ppm, 1024–2048256–512 data points were used at proton and nitrogen frequency, respectively. Tetramethylsilane (TMS) was used as a chemical shift reference for ^{1}H and calibrated at 0.00 ppm. The water suppression and polynomial base-line correction were applied. Because of the existence of high concentrations of urea in both samples, a strong peak at 5.78 ppm was visible.

3. Results

3.1. Formation of amyloid-like structures at low concentrations of urea

ThT assay is an accurate technique for detecting amyloid-like fibrillar structures. This dye is capable of binding to aggregates with β-sheet structure and, as a consequence, its fluorescence intensity increases significantly with a maximum at 490 nm [19,20]. 15 samples were prepared containing 2.0 mg/ml (60 μM) lipase in 50 mM Tris-HCl, pH 8.0 and urea concentrations ranging from 1.0 to 8.0 M with 0.5 M steps. The samples were incubated at 25 °C for 24 h and then subjected to the ThT assay. As indicated in Fig. 1a, lipase samples containing 1.0 to 3.0 M urea were capable of increasing ThT fluorescence intensity significantly, while for the samples at higher urea concentrations no significant increase in ThT fluorescence intensity was detected. The blank subtracted values of ThT fluorescence intensity at 490 nm are almost equal to zero for the samples in 3.5 M to 8.0 M urea, but these values are remarkably high for samples at lower urea concentrations (Fig. 1b).

Congo red binding assay is another method for the detection of amyloid-fibril like structures [21]. The binding of the dye to aggregates with a β-sheet structure causes a redshift of its peak of maximum absorption and a shoulder in its spectrum and a maximum peak at 540 nm in the difference spectrum [22]. The CR binding assay was performed for the 15 samples. The characteristic redshift was detected only in the samples containing 1.0 to 2.5 M urea (Fig. 1c–d). The peak at 540 nm in the difference spectra, obtained by subtracting the absorbance values of protein only and CR only from the absorbance values of CR with protein, was also obtained in the same samples. A noticeable decrease in the 540 nm peak was found after decreasing urea concentration from 2.5 M to 3.0 M (Fig. 1e). This decrease indicates that the dye is not capable of binding to lipase at urea concentrations higher than 2.5 M and shows that amyloid-like structures are not detectable in these samples.

Hence, the ThT and CR assays indicate that β-sheet containing aggregates are present only at low urea concentrations, up to 2.5–3.0 M,

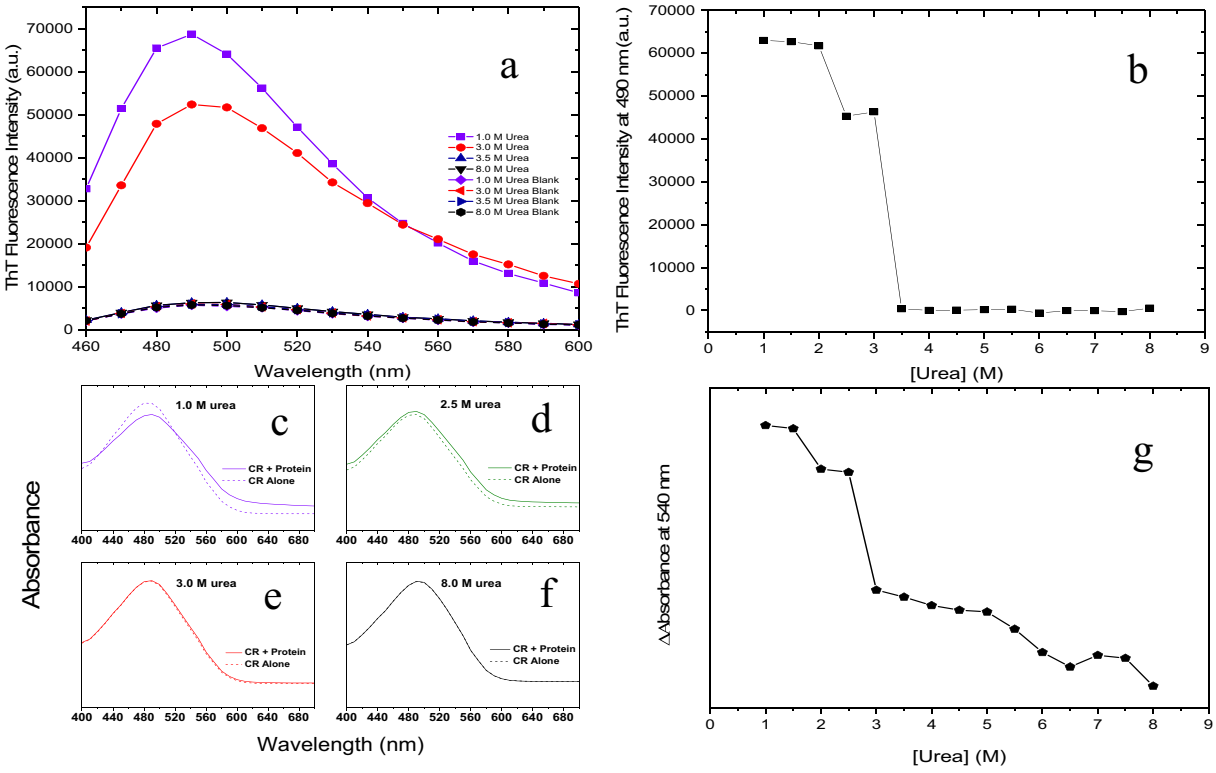

Fig. 1. (A) ThT fluorescence spectra in the presence and absence of lipase in 1.0, 3.0, 3.5, and 8.0 M urea, shown here as representative spectra. (B) ThT fluorescence intensity at 490 nm of all lipase samples in 1.0–8.0 M urea. The corresponding ThT fluorescence value recorded in the absence of protein was subtracted in all cases. (C–F) CR absorbance spectra in the presence and absence of lipase in 1.0, 2.5, 3.0 and 8.0 M urea, shown here as representative spectra. (G) Difference Absorbance values (ΔAbsorbance) at 540 nm calculated with Eq. (1) for all lipase samples in 1.0–8.0 M urea.

under the conditions of protein concentration, pH and temperature explored here. Transmission electron microscopy images have shown that aggregates forming under these conditions are fibrillar and have a morphology and diameter typical of amyloid-like fibrils [13,14].

3.2. Formation of aggregates without amyloid properties at higher urea concentrations

The apparent hydrodynamic diameters (D_h) of lipase species in the whole range of urea concentration were detected using Dynamic light scattering (DLS) (Fig. 2a–d). The size distributions by light scattering intensity of the samples from 4.5 M to 8.0 M urea are characterized by two peaks, at ca. 10–20 nm and ca. 100–300 nm, respectively. Because the intensity of the scattered light correlates with the second power of a particle mass and sixth power of its diameter, the second species detected here is quantitatively irrelevant [23]. The mean D_h of lipase in 8.0 M urea was found to be 15.7 ± 1.8 nm. This value is in agreement with that obtained in a previous investigation [9] and with the predicted value for an unfolded protein with the same number of residues as our lipase, i.e. 11.7 ± 3.6 nm [24]. These monomeric species were not detectable in the lipase samples at urea concentrations lower than 4.5 M. The distributions of D_h values for these samples indicated the dominance of particles larger than monomeric species with no constant size.

These results are in agreement with the change of light scattering intensity (Fig. 2e) and turbidity (Fig. 2f) with urea concentration. Indeed, the light scattering intensity and turbidity values are small at the high concentrations of urea (4.5–8.0 M), indicating the predominance of monomeric particles under these conditions. The values at 4.0 M urea are higher and the monomers are no longer detectable in the size distributions because they are overshadowed by large particles. The values are even higher at lower urea concentrations (1.0–3.5 M), showing the existence of large aggregates.

Importantly, the three techniques used here to monitor aggregates indicate the persistence of these species from 0.0 to 4.0 M urea (Fig. 2), whereas the ThT and CR assays indicate the presence of β-sheet containing aggregates up to 2.5–3.0 M urea (Fig. 1). This discrepancy reveals the existence of lipase aggregates that do not bind ThT/CR, and are therefore devoid of ordered β-sheet structure, at 3.5–4.0 M urea.

3.3. Intrinsic fluorescence reveals another transition at high urea concentrations

Because of the existence of two tryptophan residues in the lipase sequence, tryptophan fluorescence emission was used as an intrinsic probe for identifying protein conformational changes during the urea titration. Two peaks with maximum emission at 330 nm and 351 nm were detected in the emission spectra at the lowest urea concentrations (Fig. 3a). The intensity of both peaks is almost equal in the samples containing 1.0–2.0 M urea, but with increasing the urea concentration the rise in the intensity of the peak at 351 nm is more noticeable. This behaviour is more evident by plotting the ratio of the fluorescence intensity values at 351 and 330 nm (F_{351}/F_{330}) versus urea concentration, with a large multistep transition occurring between ca. 2.0–2.5 M and 6.0–7.0 M urea (Fig. 3b). This transition starts approximately when the β-sheet aggregates decrease in population, but does not end when such aggregates are no longer populated (3.0–3.5 M urea) or when the non-β aggregates are no longer populated (4.5 M urea). It ends at higher urea concentration, i.e. ca. 6.0–7.0 M urea, indicating a different type of transition that is not superimposable to that observed with all other probes monitoring aggregation. The transition appears to be multi-state, rather than two-state, as indicated by its large shape and the apparent changes of slope in the various regions of the transition. Indeed, it covers the transitions from (i) the β-sheet aggregate to the non-β aggregate, (ii) from the non-β aggregate to the monomeric state at 4.5 M urea and (iii) from this state to another one at high urea concentrations.

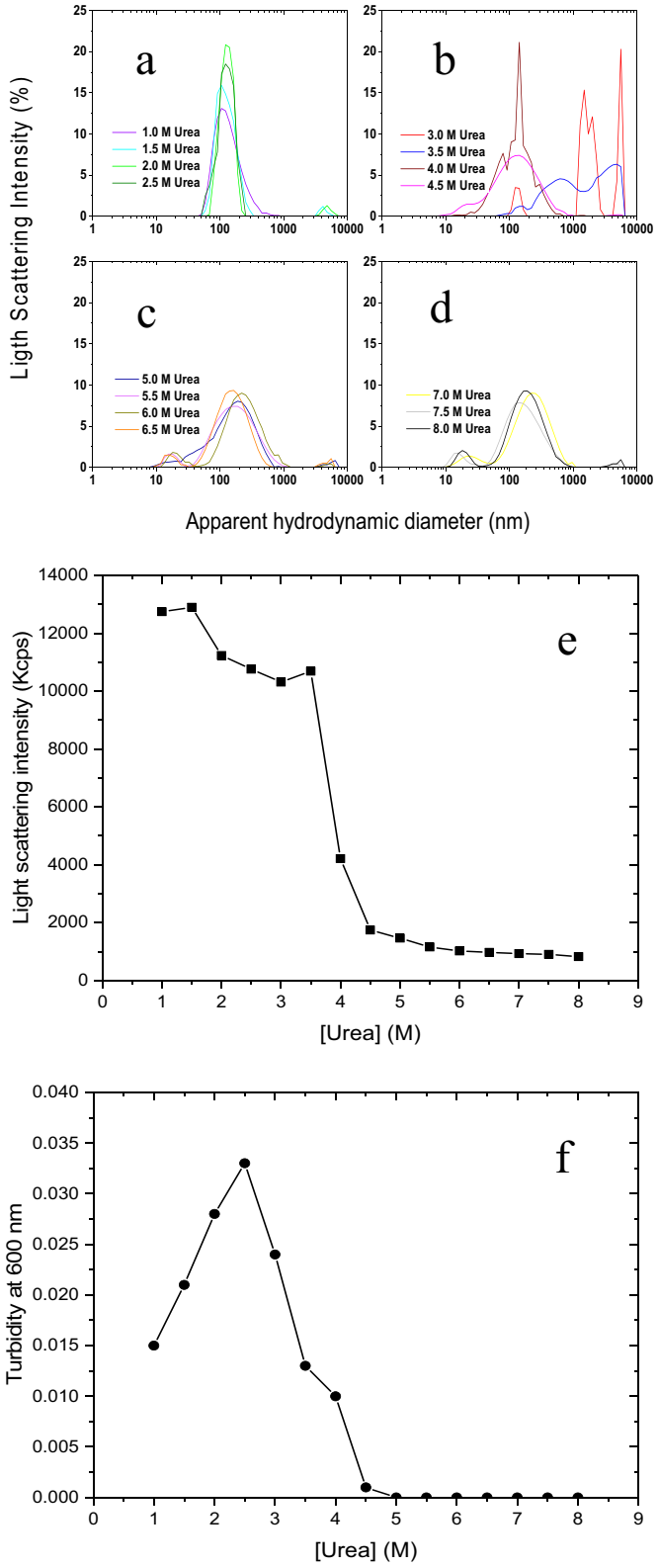

Fig. 2. (A–D) Size distributions of lipase samples in 1.0–8.0 M urea. (E, F) Light scattering intensity in kilocounts per second (Kcps) (E) and turbidity at 600 nm (F) of lipase samples at urea concentrations ranging from 1.0 M to 8.0 M.

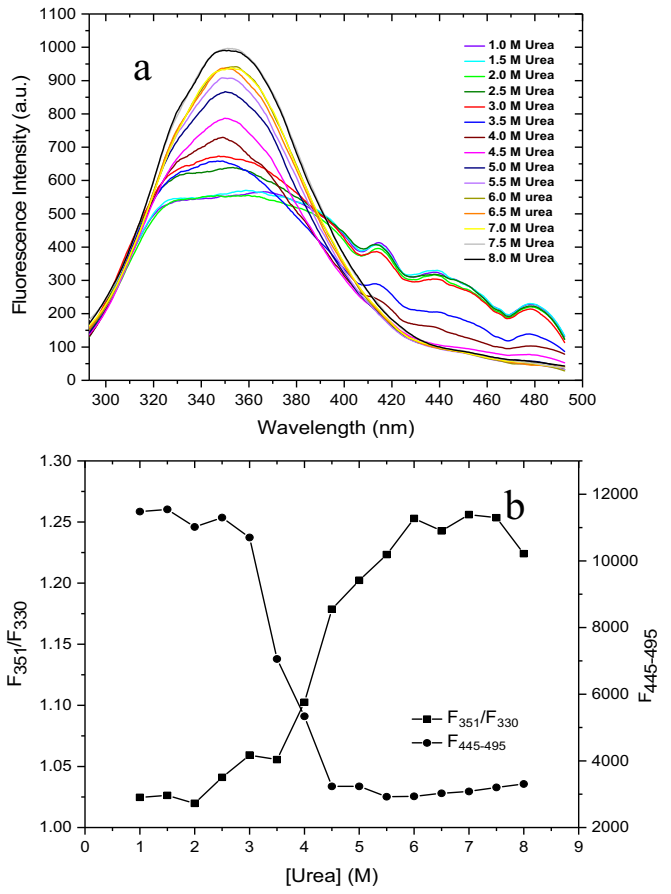

Fig. 3. (A) Intrinsic fluorescence spectra of lipase at different concentrations of urea, from 1.0 M to 8.0 M. (B) The area under the 445–495 nm wavelength region ($F_{445–495}$) and the ratio of fluorescence intensity values at 351 and 330 nm (F_{351}/F_{330}) as a function of urea concentration.

Furthermore, the area under the same fluorescence spectra in the 445–495 nm wavelength range ($F_{445–495}$) decreases by increasing urea concentration (Fig. 3a, b). The fluorescence emission in this spectral window does not arise from tryptophan fluorescence [25], and is rather attributable to the light scattered by the aggregates. It is not therefore surprising that the plot of $F_{445–495}$ versus urea concentration is close to that obtained with light scattering intensity or turbidity, with high values in 0.0–3.0 M urea, small values in 4.5–8.0 M urea and a transition between these two regions (Fig. 3b). The two transitions probed with F_{351}/F_{330} and $F_{445–495}$ using the same experimental set of lipase samples are not superimposable, as the former ends at higher urea concentrations than the latter (Fig. 3b). It is therefore clear that a new conformational transition is probed by intrinsic tryptophan fluorescence after 4.5 M urea, when the protein has acquired a monomeric state.

3.4. Detection of solvent-exposed hydrophobic patches in urea titration

The 8-Anilinonaphthalene-1-sulfonic acid (ANS) binding assay was used for studying the solvent-exposure of hydrophobic patches of lipase species in different concentrations of urea. ANS fluorescence intensity enhancement and blueshift occur as a result of the binding of this small dye to the hydrophobic regions of the protein surface [26,27]. The ANS fluorescence intensity in the presence of lipase was found to increase in all conditions relative to the corresponding solutions in the absence of protein, indicating an ability of the protein to bind ANS in the whole range of urea concentration (Fig. 4a). However, the blueshift was not detected in all cases: the wavelength of maximum emission (λ_{max}) is the lowest in 1.0 M urea (maximum blueshift) and then increases progressively until 3.5 M urea to remain stable until 8.0 M urea (Fig. 4a, B). Similarly, the ANS fluorescence intensity in 1.0 M urea at 450–490 nm ($F_{450–490}$) is the highest, then decreases progressively up to 3.0 M urea and remains stable (Fig. 4a, b). However, after 5.5 M urea, the ANS fluorescence intensity in this region starts to

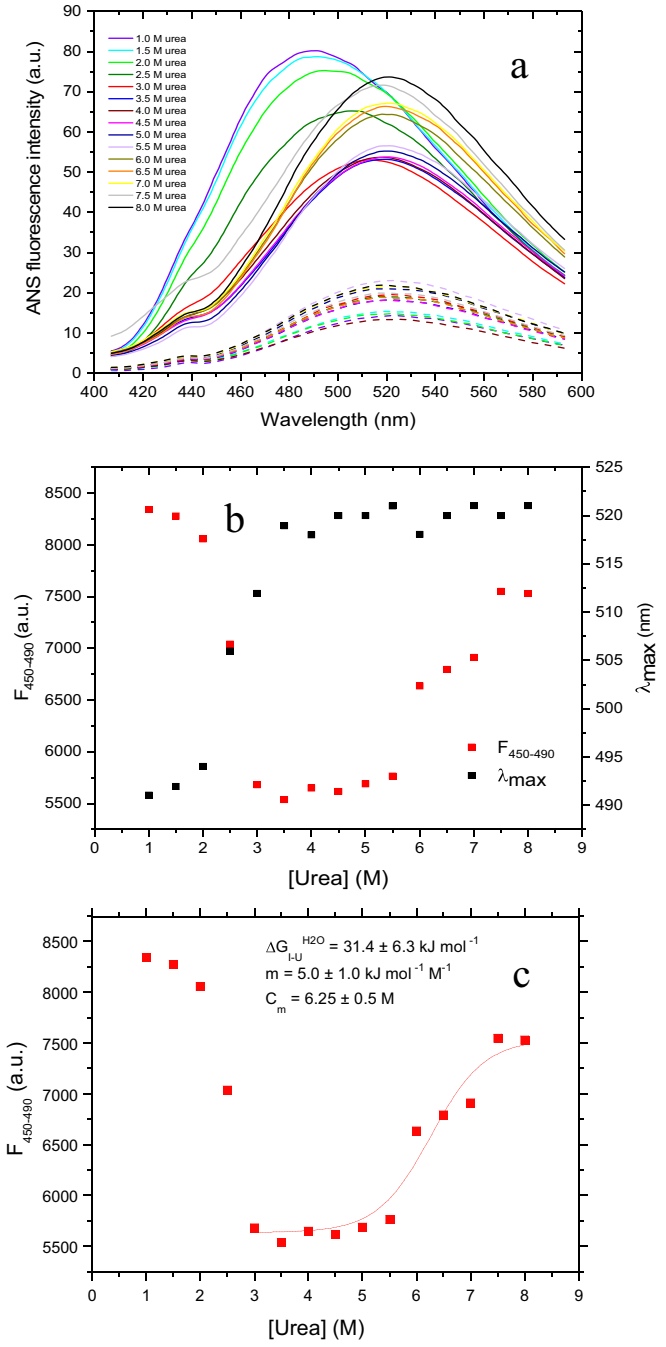

Fig. 4. ANS fluorescence spectra in the presence (continuous lines) and absence (dashed lines) of lipase in 1.0 to 8.0 M urea. Spectra with the same colour refer to the same urea concentration. (B) The area under the 450–490 nm wavelength region ($F_{450–490}$) and the wavelength of maximum emission (λ_{max}) of ANS fluorescence at various urea concentrations. (C) The same plot of $F_{450–490}$ versus urea concentration shown in (B) fitted with a two state model [28].

increase progressively again to reach a new stable value at 7.5 and 8.0 M urea (Fig. 4b).

The ANS analysis indicates two major transitions: one between 2.0 M and 3.0–3.5 M urea, similar to that observed with the ThT and CR assays between a β-sheet containing and a non-β aggregate, and one between 5.5 M urea and 7.5 M urea, similar to the last part of the transition monitored with intrinsic fluorescence that is silent to all probes for aggregation, therefore corresponding to a transition between two different monomeric states (Fig. 4b). In other words, the ANS analysis is indicative of three different conformational states in urea titration: a first state at ca. 1.0–2.0 M urea with a small value of λ_{max} and a high value of $F_{450–490}$, corresponding largely to the β-sheet containing aggregates; a second state at ca. 3.0–5.5 M urea with a large value of λ_{max} (no blueshift) and the smallest value of $F_{450–490}$, corresponding to both the aggregates devoid of β-sheet structure and the subsequent monomeric conformational state (appearing indistinguishable with the assay); a third state at 7.5–8.0 M urea without ANS blueshift and high values of $F_{450–490}$, corresponding to the most unfolded state of lipase (Fig. 4b).

These results indicate the maximum solvent-exposure of hydrophobic clusters on the protein surface at low urea concentrations, when lipase forms structured aggregates (maximum blueshift and fluorescence increase), that a much lower number of hydrophobic clusters are exposed at the highest urea concentrations (no blueshift, smaller fluorescence increase), and that an even lower number of exposed hydrophobic clusters are present at intermediate urea concentrations values when the non-β aggregate and first monomeric state are populated (no blueshift, minimal fluorescence increase), indicating a large burial of hydrophobic clusters in this case.

Since the two monomeric conformational states populated at moderate and high urea concentrations, respectively, can be distinguished on the grounds of different ANS fluorescence values and the transition appears to be cooperative, we attempted to fit the data points to a two-state model [28], leading to an m value of 5.0 ± 1.0 kJ mol^{-1} M^{-1}, a free energy change of 31.4 ± 6.3 kJ mol^{-1} and a transition midpoint of 6.25 ± 0.5 M (Fig. 4c).

3.5. Characterization of the four conformational states populated in urea titration

In order to characterize the secondary structures of the various conformational states of lipase populated in the urea titration, far-UV Circular dichroism (CD) was used [29]. Because of the presence of urea in the samples, an ultrafine cuvette was used to avoid the high absorbance of urea in the far-UV region of light. The spectra in 7.5 M, 4.5 M, 3.5 M and 2.0 M urea were reported as representative spectra of the largely unstructured monomer, partially folded monomer, non-β aggregate and β-sheet aggregate, respectively (Fig. 5a). The spectrum in 2.0 M urea features a negative peak at ca. 215 nm, indicating the presence of extensive β-sheet structure. The spectrum in 7.5 M urea is flat at high wavelength values and have a negative peak at ca. 195–200 nm, indicating a substantially unordered secondary structure. The spectrum in 3.5 M urea indicates a largely α-helical structure, with two negative peaks at ca. 208 nm and ca. 222 nm, whereas the spectrum at 4.5 M urea is intermediate between those recorded in 3.5 M and 7.5 M urea.

The enzymatic activity of representative lipase samples was also measured to determine if any lipase species which forms during its titration are native-like and active or not. The measured activity of the folded state of lipase (0.0 M urea), generated with its specific foldase as previously reported (2) was normalized to 100%. Enzymatic activity was not detected for any of the lipase samples (Fig. 5b), indicating that none of the four conformational states populated during the urea titration has a native-like structure.

The two monomeric conformational states of lipase in 4.5 M and 7.5 M urea were further characterized using acrylamide quenching of tryptophan fluorescence, as a probe of solvent-exposure of its tryptophan residues [30,31]. The tryptophan fluorescence spectra of lipase in 4.5 M and 7.5 M urea were recorded at different acrylamide concentrations and the ratio of total fluorescence in the absence and presence of acrylamide (F_0/F) was plotted versus acrylamide concentration for both lipase samples (Fig. 5c). The computed K_{sv} values, corresponding to the slopes of the plots, were found to be 6.75 ± 0.13 M^{-1} and 14.07 ± 0.11 M^{-1} for the lipase samples in 4.5 M and 7.5 M urea, respectively (Fig. 5c). The K_{sv} value obtained in 7.5 M urea is lower than that of free tryptophan, which is approximately 19–20 M^{-1} [32–34], indicating that the two tryptophan residues of lipase in this conformational state are, on average, largely solvent exposed, but to an extent lower than

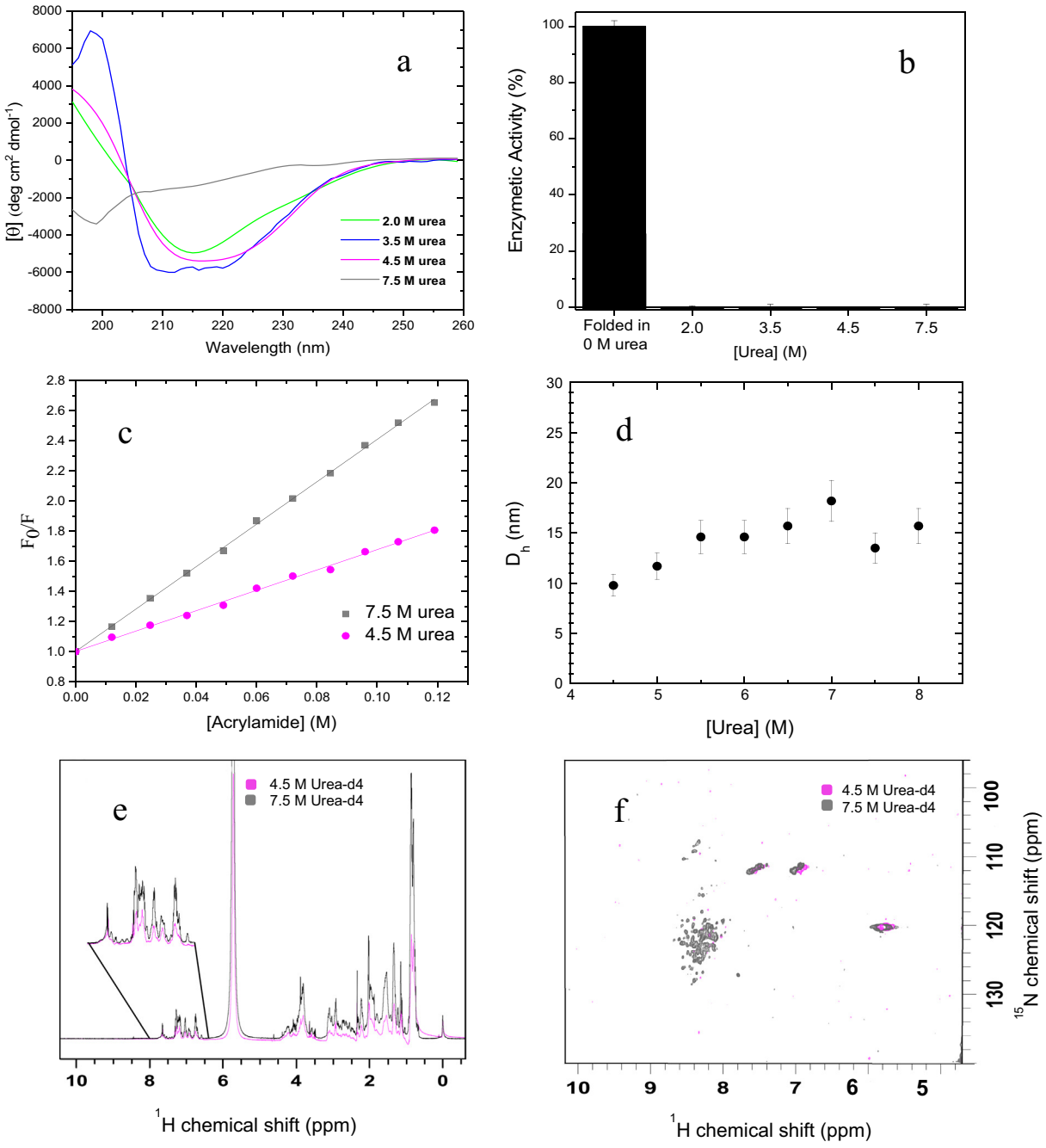

Fig. 5. (A) Far-UV CD spectra of lipase in 2.0 M, 3.5 M, 4.5 M and 7.5 M urea. (B) Enzymatic activity of lipase in 2.0 M, 3.5 M, 4.5 M and 7.5 M urea. The activity in 0 M urea for the protein refolded as described previously [12] is also reported as a positive control. (C) Stern–Volmer plots of lipase in 4.5 M and 7.5 M urea using acrylamide as a quencher. (D). Apparent D_h of lipase versus urea concentration (4.5–8.0 M) obtained with DLS. (E) 1D spectra and (F) 2D ^{15}N-^{1}N-HSQC spectra of lipase acquired in 4.5 M and 7.5 M urea-d4 in D_2O.

that of a fully unstructured protein. By contrast, the K_{sv} value obtained in 4.5 M urea is significantly lower, revealing largely buried tryptophan residues in this conformational state.

A close inspection of the size distributions by light scattering intensity obtained with DLS, and converted into size distributions by volume, reveals that the 4.5 M and 8.0 M urea states have D_h values of 9.8 ± 1.1 nm and 15.7 ± 1.8 nm, respectively (Fig. 5d). As mentioned earlier, the latter value in 8.0 M urea is compatible with that of a fully unfolded protein of 317 residues, i.e. 11.7 ± 3.6 nm [24], whereas the former value in 4.5 M urea reveals a significantly more compact state, yet larger than that expected for a folded protein of this size, i.e. 5.05 ± 1.6 nm [24].

We then analyzed the 1D and 2D ^{15}N-^{1}H-HSQC Nuclear magnetic resonance (NMR) spectra of ^{15}N-enriched lipase samples in 4.5 M and 7.5 M urea-d4 in D_2O (Fig. 5e, f). The 1D ^{1}H spectra showed, for both samples, a large number of peaks clustered between 0.5 and 4.5 ppm and between 6.5 and 8.0 ppm, arising from aliphatic/CHα and aromatic ^{1}H atoms, respectively (Fig. 5e). Such a high level of chemical shift clustering indicates that the protein is largely non-native in both cases, with loss of peaks typical of a folded protein. A close inspection of the two spectra reveals, however, a higher level of line-broadening and intensity decrease in 4.5 M urea (Fig. 5e, zoom). The two spectra are indeed fully comparable as they were normalized for the same intensity of the ^{1}H peak arising from tetramethylsilane at 0.0 ppm, added to the two samples to the same final concentration. The large peak at 5.78 ppm visible in both spectra arises from urea-d4 that has exchanged its D atoms with the H atoms coming from the D_2O solvent as impurities.

The 2D ^{15}N-^{1}H-HSQC NMR spectra feature peaks with very low intensity as they arise from a very small population of ^{15}N-^{1}H amide

groups that are in equilibrium with a large population of ^{15}N-^{1}D amides that are, by contrast, invisible in the spectra (Fig. 5f). In 7.5 M urea-d4, backbone amides, glycine amides and side chain amides (Asn and Gln residues) are clearly detectable with marked line-sharpening. The poor degree of chemical shift dispersion of the non-glycine backbone amides indicates a high level of unfolding of the polypeptide chain. A similar level of chemical shift dispersion was also detectable in 4.5 M urea-d4, but in this case, a severe line-broadening is apparent, where only a small number of backbone amides are visible. This reveals a significant level of intramolecular interactions where the peaks appear to be neither fully folded nor fully unfolded. Control experiments with DLS and far-UV CD carried out on the same sample analyzed with NMR confirmed the monomeric state of this conformation state (data not shown).

4. Discussion

Generally, lipases are active at the oil–*water* interface and *transform* between *two* conformations, an open (active) and a closed (inactive) *one*. The active form occurs in the presence of hydrophobic surfaces that increase the enzyme activity [17,35]. The lipase studied here has a very high aggregation propensity under conditions in which the protein is not correctly folded [8–10]. After dialysis at 25 °C of a protein sample containing 0.4 mg/ml lipase in 8 M urea at pH 8.0, to remove the denaturant and obtain conditions expected to promote its folding, the protein was found to be aggregated into amyloid-like fibrils, appearing fibrillar under transmission electron microscopy, binding the amyloid diagnostic dyes ThT and CR and containing a significant quantity of β-sheet structure, as detected with far-UV CD and FTIR spectroscopies [8]. After a ten-fold dilution of a similar protein sample containing 4.0 mg/ml lipase in 8.0 M urea at pH 8.0, to reach final urea concentrations of 0.8–2.4 M and pH values ranging from neutral to 3.5 units higher than its isoionic point, the protein was found to bind ThT by the time the first data point was acquired (after a few seconds), indicating an extremely rapid aggregation process that predominates kinetically over that of folding [9,10].

In the present study it was confirmed that the protein forms amyloid-like aggregates from small to moderate concentrations of urea (Fig. 6). ThT-positive, CR-positive and β-sheet containing amyloid-like aggregates are detected, after 24 h incubation at a lipase concentration of 2 mg/ml, up to 3.0 M urea. Higher concentrations of urea destabilise the aggregates or slow down their process of formation to an extent sufficient to make them undetectable after 24 h. This is due to the ability of urea to destabilise any non-covalent interaction within proteins, including the hydrogen bonding network and hydrophobic interactions required for amyloid fibril formation [36].

How can the very high aggregation propensity of lipase be explained? An algorithm designed to quantify the aggregation propensity of proteins in their unfolded state (the first version of Zyggregator) indicates that unfolded lipase has an aggregation propensity higher than average over a group of proteins of the same length. However, such a deviation from the average is not very large: a Z^{agg} value of 0.184 was determined for lipase and a value of -0.25 ± 0.82 (mean ± standard deviation) was obtained for the whole human proteome within the same length interval of 300–350 residues [37,38]. The Z^{agg} value of lipase is, therefore, within one standard deviation from the mean of the group of proteins with comparable length from the whole human proteome. The difference is even more modest by considering the other parameters of aggregation propensity: 0.0221 vs 0.015 for fpeaks, 5.571 ± 2.070 vs 5 for L^{peaks}, 0.0534000 vs 0.05 for $S^{agg}/L^{protein}$, 2.42 vs 2.7 for S^{agg}/N^{peaks}. It is therefore clear that the very high aggregation propensity of unfolded lipase does not arise only from its sequence.

Concentrations of urea sufficiently high to prevent the formation of amyloid-like fibrils under the conditions explored here (equal to or higher than 3.0 M), does not lead to the formation of a largely unfolded monomeric protein (Fig. 6). The titration discloses aggregates with α-helical structure (3.0–4.0 M urea) and then a monomeric denatured state, but still enriched with α-helical secondary structure (4.5–5.5 M). It is not until a urea concentration of 7.0–8.0 M that a predominantly unfolded monomeric state appears to be largely populated (Fig. 6). Hence, this protein is able to populate a stable partially folded state, which unfolds only at high urea concentrations.

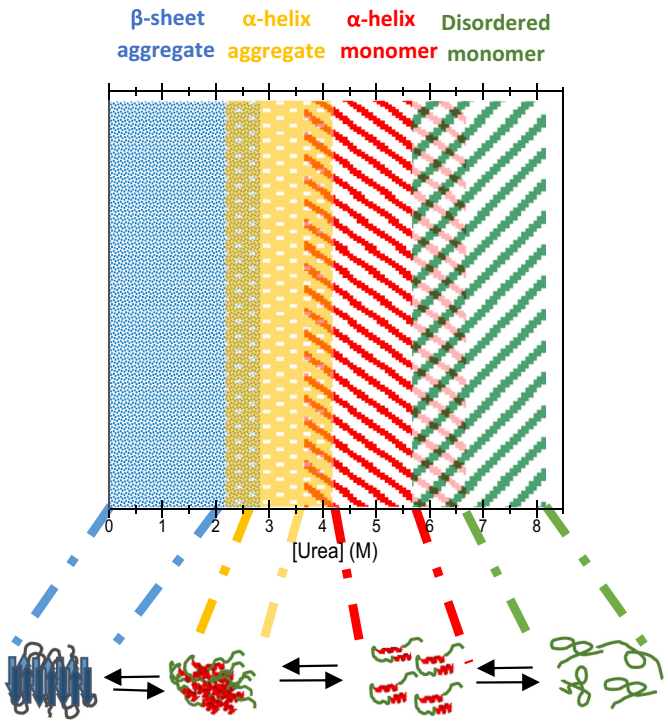

Fig. 6. Schematic figure indicating the detected species of lipase in 1.0 to 8.0 M urea and their transitions under the conditions explored here (2.0 mg/ml (60 μM) lipase, 50 mM Tris-HCl, pH 8.0, 25 °C, 24 h).

The conformational state populated at moderate urea concentrations (4.5 M) is monomeric (as shown by DLS, SLS and turbidimetry), more compact than the fully unfolded state (as indicated by its D_h estimated with DLS), significantly α-helical (far-UV CD), has very weak exposure of hydrophobic residues (ANS-derived fluorescence), partially buried tryptophan residues (low F_{351}/F_{330} and K_{SV} values), significant level of intramolecular interactions in the absence of a fully folded structure (NMR) and has no enzymatic activity (indicating a non-native state). The transition from this conformational state to the fully unfolded state is cooperative, with an a urea *m* value of 5.0 ± 1.0 kJ mol^{-1} M^{-1}, which is lower than that expected for a fully folded protein of 317 residues [39], but larger than those observed for loosely packed partially folded states that typically undergo large uncooperative transitions. Its stability relative to the unfolded state ($\Delta G_{I\text{-}U}^{H2O}$) is 31.4 ± 6.3 kJ mol^{-1} and the transition midpoint is 6.25 ± 0.5 M urea, which are quite high for a partially folded state.

Is the high stability of this α-helical compact denatured state the factor responsible for the high aggregation propensity of the lipase protein studied here? A number of observations suggest that this is the case. First, it has a large tendency to self-assemble into α-helical enriched aggregates, as shown by its behaviour as the urea concentration decreases from 4.5 M to 3.0–4.0 M, that is sufficiently low to allow intermolecular interactions between α-helical containing monomers, but sufficiently high to inhibit the formation of the more structured cross-β amyloid. As urea concentration decreases further, these α-helical assemblies are likely to be further stabilized and allow the formation of the β-sheet aggregates typical of amyloid.

Second, although the role of α-helical structure in amyloid fibril formation is complex, it has recently been clarified. Partially folded

states containing α-helical structure are intermediates in the formation of amyloid; this is not because α-helical secondary structure promotes amyloid aggregation per se, but because α-helices are generally amphipathic and their formation leads to the generation of hydrophobic surfaces that allow such helices from different protein molecules to interact and initiate the process of self-assembly [40–43]. Moroever, when a key region of the sequence that plays a crucial role in amyloid formation adopts stable α-helical structure, this type of secondary structure is protective against aggregation and its further stabilization by mutations counteracts amyloid aggregation [44–48]. However, it can be aggregation-promoting for non-amyloidogenic initially unstructured stretches [49]. This seems to be the case also for lipase, as the F171E mutation within the most important aggregation promoting region (residues 160–172) inhibits aggregation significantly, due to its ability to decrease and increase the β-sheet and α-helical propensities, respectively [9]. However, the typical α-helical CD spectrum of the partially folded state of lipase indicates that such a structure extends far beyond this region of the sequence, representing therefore a promoting factor for β-aggregation.

5. Conclusions

The urea-unfolded lipase from *Pseudomonas* sp. studied here was previously shown to have a unique behaviour to convert to amyloid-like structures and forms these β-sheet aggregate rapidly, without any lag phase in the absence of denaturants. Our present analysis shows that this observation in not attributable to a high intrinsic sequence-specific aggregations propensity. Rather, the existence of a stable partially folded state can explain the high prepotency of this protein to form amyloid-like structures. This α-helical state promotes amyloid formation because it has an amphipathic nature and generates extended hydrophobic surfaces that are essential for their formation in a rapid manner. This feature leads to the initiation of the process of self-assembly and to the interaction of different lipase monomers. These results suggest that at least for some proteins with high propensity to form amyloid-like structures, the conversion to a stable partially folded state promotes the fibrillation process and facilitates the conversion of the monomers to β-sheet aggregates. In addition, elucidating the mechanisms by which this lipase converts into amyloid-like fibrils provides suggestions of how other proteins with similar extreme behaviour may form amyloid-like structures and help the rational modulation of the aggregation process in this group of enzymes.

CRediT authorship contribution statement

Conception and design of study:
Fabrizio Chiti
Acquisition of data:
Minoo Qafary, Matteo Ramazzotti
Analysis and/or interpretation of data:
Fabrizio Chiti, Ali Akbar Moosavi-Movahedi, Minoo Qafary
Drafting the manuscript:
Fabrizio Chiti, Minoo Qafary
Revising the manuscript critically for important intellectual content:
Fabrizio Chiti, Khosro Khajeh, Ali Akbar Moosavi-Movahedi
Approval of the version of the manuscript to be published (the names of all authors must be listed):
Minoo Qafary, Khosro Khajeh, Matteo Ramazzotti, Ali Akbar Moosavi-Movahedi, Fabrizio Chiti

Declaration of competing interest

The authors declare that they have no conflict of interest.

Acknowledgments

This work was supported by the Research Council of Tehran University, University of Florence (Fondi di Ateneo), Iran National Science Foundation (INSF) and the Research Council of Tarbiat Modares University.

Funding

This work was supported by the grant provided by "Research Council of Tehran University and Iran National Science Foundation (INSF)" assigned to Ali Akbar Moosavi-Movahedi, by the grant provided by "Fondi di Ateneo of University of Florence" assigned to Fabrizio Chiti and the grant provided by "Research Council of Tarbiat Modares University" assigned to Khosro Khajeh.

Availability of data and material

All data generated or analyzed during this study are included in this published article.
Code availability: Not applicable.
Ethics approval: Not applicable.
Consent to participate: Not applicable.
Consent for publication: Not applicable.

References

[1] F. Chiti, C.M. Dobson, Protein misfolding, amyloid formation, and human disease: a summary of progress over the last decade, Annu. Rev. Biochem. 86 (2017) 27–68, https://doi.org/10.1146/annurev-biochem-061516-045115.
[2] T.R. Jahn, S.E. Radford, Folding versus aggregation: polypeptide conformations on competing pathways, Arch. Biochem. Biophys. 469 (1) (2008) 100–117, https://doi.org/10.1016/j.abb.2007.05.015.
[3] S. Ventura, A. Villaverde, Protein quality in bacterial inclusion bodies, Trends Biotechnol. 24 (4) (2006) 179–185, https://doi.org/10.1016/j.tibtech.2006.02.007.
[4] I. Cherny, E. Gazit, Amyloids: not only pathological agents but also ordered nanomaterials, Angew. Chem. Int. Ed. 47 (22) (2008) 4062–4069, https://doi.org/10.1002/anie.200703133.
[5] D. Balchin, M. Hayer-Hartl, F.U. Hartl, In vivo aspects of protein folding and quality control, Science 353 (6294) (2016), aac4354, https://doi.org/10.1126/science.aac4354.
[6] J. Labbadia, R.I. Morimoto, The biology of proteostasis in aging and disease, Annu. Rev. Biochem. 84 (2015) 435–464, https://doi.org/10.1146/annurev-biochem-060614-033955.
[7] D.J. Selkoe, J. Hardy, The amyloid hypothesis of Alzheimer's disease at 25 years, EMBO Mol. Med. 8 (6) (2016) 595–608, https://doi.org/10.15252/emmm.201606210.
[8] M. Monsef Shokri, S. Ahmadian, F. Bemporad, K. Khajeh, F. Chiti, Amyloid fibril formation by a normally folded protein in the absence of denaturants and agitation, 20 (4) (2013) 226–232, https://doi.org/10.3109/13506129.2013.830246.
[9] F. Rashno, K. Khajeh, C. Capitini, R.H. Sajedi, M.M. Shokri, F. Chiti, Very rapid amyloid fibril formation by a bacterial lipase in the absence of a detectable lag phase, Biochim. Biophys. Acta Protein Proteomics 1865 (6) (2017) 652–663, https://doi.org/10.1016/j.bbapap.2017.03.004.
[10] F. Rashno, K. Khajeh, B. Dabirmanesh, R.H. Sajedi, F. Chiti, Insight into the aggregation of lipase from Pseudomonas sp. using mutagenesis: protection of aggregation prone region by adoption of α-helix structure, Protein Eng. Des. Sel. 31 (11) (2018) 419–426, https://doi.org/10.1093/protein/gzz003.
[11] N. Akbari, K. Khajeh, N. Ghaemi, Z. Salemi, Efficient refolding of recombinant lipase from Escherichia coli inclusion bodies by response surface methodology, Protein Expr. Purif. 70 (2) (2010) 254–259, https://doi.org/10.1016/j.pep.2009.10.009.
[12] N. Akbari, K. Khajeh, S. Rezaie, S. Mirdamadi, M. Shavandi, N. Ghaemi, High-level expression of lipase in Escherichia coli and recovery of active recombinant enzyme through in vitro refolding, Protein Expr. Purif. 70 (1) (2010) 75–80, https://doi.org/10.1016/j.pep.2009.08.009.
[13] K.-E. Jaeger, T. Eggert, Lipases for biotechnology, Curr. Opin. Biotechnol. 13 (4) (2002) 390–397, https://doi.org/10.1016/S0958-1669(02)00341-5.
[14] F. Hasan, A.A. Shah, A. Hameed, Industrial applications of microbial lipases, Enzym. Microb. Technol. 39 (2) (2006) 235–251, https://doi.org/10.1016/j.enzmictec.2005.10.016.
[15] J.C. Dos Santos, H.L. Bonazza, L.J. de Matos, E.A. Carneiro, O. Barbosa, R. Fernandez-Lafuente, L.R. Gonçalves, H.B. de Sant'Ana, R.S. Santiago-Aguiar, Immobilization of CALB on activated chitosan: application to enzymatic synthesis in supercritical and near-critical carbon dioxide, Biotechnol. Rep. 14 (2017) 16–26, https://doi.org/10.1016/j.btre.2017.02.003.
[16] T. Carvalho, A.d.S. Pereira, R.C. Bonomo, M. Franco, P.V. Finotelli, P.F. Amaral, Simple physical adsorption technique to immobilize Yarrowia lipolytica lipase purified by different methods on magnetic nanoparticles: adsorption isotherms and

thermodynamic approach, Int. J. Biol. Macromol. (2020)https://doi.org/10.1016/j.ijbiomac.2020.05.174.
[17] N.S. Rios, B.B. Pinheiro, M.P. Pinheiro, R.M. Bezerra, J.C.S. dos Santos, L.R.B. Gonçalves, Biotechnological potential of lipases from Pseudomonas: sources, properties and applications, Process Biochem. 75 (2018) 99–120, https://doi.org/10.1016/j.procbio.2018.09.003.
[18] N. Mollania, K. Khajeh, B. Ranjbar, F. Rashno, N. Akbari, M. Fathi-Roudsari, An efficient invitro refolding of recombinant bacterial laccase in Escherichia coli, Enzym. Microb. Technol. 52 (6–7) (2013) 325–330, https://doi.org/10.1016/j.enzmictec.2013.03.006.
[19] H. Levine III, Thioflavine T interaction with synthetic Alzheimer's disease β-amyloid peptides: detection of amyloid aggregation in solution, Protein Sci. 2 (3) (1993) 404–410, https://doi.org/10.1002/pro.5560020312.
[20] M.V. Khan, G. Rabbani, M. Ishtikhar, S. Khan, G. Saini, R.H. Khan, Non-fluorinated cosolvents: a potent amorphous aggregate inducer of metalloproteinase-conalbumin (ovotransferrin), Int. J. Biol. Macromol. 78 (2015) 417–428, https://doi.org/10.1016/j.ijbiomac.2015.04.021.
[21] M.V. Khan, M. Ishtikhar, G. Rabbani, M. Zaman, A.S. Abdelhameed, R.H. Khan, Polyols (glycerol and ethylene glycol) mediated amorphous aggregate inhibition and secondary structure restoration of metalloproteinase-conalbumin (ovotransferrin), Int. J. Biol. Macromol. 94 (2017) 290–300, https://doi.org/10.1016/j.ijbiomac.2016.10.023.
[22] W.E. Klunk, R.F. Jacob, R.P. Mason, Quantifying amyloid by congo red spectral shift assay, methods in enzymology, Elsevier (1999) 285–305, https://doi.org/10.1016/s0076-6879(99)09021-7.
[23] K.S. Schmitz, An Introduction to Dynamic Light Scattering by Macromolecules, Academic Press, Boston, 1990https://doi.org/10.1016/C2009-0-29091-X.
[24] D.K. Wilkins, S.B. Grimshaw, V. Receveur, C.M. Dobson, J.A. Jones, L.J. Smith, Hydrodynamic radii of native and denatured proteins measured by pulse field gradient NMR techniques, Biochemistry 38 (50) (1999) 16424–16431, https://doi.org/10.1021/bi991765q.
[25] J.R. Lakowicz, Principles of Fluorescence Spectroscopy, Springer Science & Business Media, New York, 2013https://doi.org/10.1002/9783527633500.ch1.
[26] L. Stryer, The interaction of a naphthalene dye with apomyoglobin and apohemoglobin: a fluorescent probe of non-polar binding sites, J. Mol. Biol. 13 (2) (1965) 482–495, https://doi.org/10.1016/S0022-2836(65)80111-5.
[27] G. Rabbani, E. Ahmad, N. Zaidi, S. Fatima, R.H. Khan, pH-induced molten globule state of Rhizopus niveus lipase is more resistant against thermal and chemical denaturation than its native state, Cell Biochem. Biophys. 62 (3) (2012) 487–499, https://doi.org/10.1007/s12013-011-9335-9.
[28] M.M. Santoro, D. Bolen, Unfolding free energy changes determined by the linear extrapolation method. 1. Unfolding of phenylmethanesulfonyl. alpha.-chymotrypsin using different denaturants, Biochemistry 27 (21) (1988) 8063–8068, https://doi.org/10.1021/bi00421a014.
[29] K. Thakur, T. Kaur, J. Singh, G. Rabbani, R.H. Khan, R. Hora, M. Kaur, Sauromatum guttatum lectin: spectral studies, lectin-carbohydrate interaction, molecular cloning and in silico analysis, Int. J. Biol. Macromol. 104 (2017) 1267–1279, https://doi.org/10.1016/j.ijbiomac.2017.06.123.
[30] A. Varshney, B. Ahmad, G. Rabbani, V. Kumar, S. Yadav, R.H. Khan, Acid-induced unfolding of didecameric keyhole limpet hemocyanin: detection and characterizations of decameric and tetrameric intermediate states, Amino Acids 39 (3) (2010) 899–910, https://doi.org/10.1016/j.ijbiomac.2017.06.123.
[31] G. Rabbani, E. Ahmad, M.V. Khan, M.T. Ashraf, R. Bhat, R.H. Khan, Impact of structural stability of cold adapted Candida antarctica lipase B (CaLB): in relation to pH, chemical and thermal denaturation, RSC Adv. 5 (26) (2015) 20115–20131, https://doi.org/10.1039/C4RA17093H.
[32] V. Narayanaswami, R.O. Ryan, Molecular basis of exchangeable apolipoprotein function, Biochim. Biophys. Acta Mol. Cell Biol. Lipids 1483 (1) (2000) 15–36, https://doi.org/10.1016/s1388-1981(99)00176-6.
[33] B. Pierce, D. Toptygin, B. Wendland, Pan1 is an intrinsically disordered protein with homotypic interactions, Proteins Struct. Funct. Bioinforma. 81 (11) (2013) 1944–1963 (https://dx.doi.org/10.1002%2Fprot.24342).
[34] S. Philips, In vivo release of endogenous dopamine from rat caudate nucleus by β-phenylethylamine and α, α,-dideutero-β-phenylethylamine, Life Sci. 39 (25) (1986) 2395–2400, https://doi.org/10.1016/0024-3205(86)90480-7.
[35] F.T.T. Cavalcante, F.S. Neto, I.R. de Aguiar Falcão, J.E. da Silva Souza, L.S. de Moura Junior, P. da Silva Sousa, T.G. Rocha, I.G. de Sousa, P.H. de Lima Gomes, M.C.M. de Souza, Opportunities for improving biodiesel production via lipase catalysis, Fuel 119577 (2020)https://doi.org/10.1016/j.fuel.2020.119577.
[36] G. Rabbani, I. Choi, Roles of osmolytes in protein folding and aggregation in cells and their biotechnological applications, Int. J. Biol. Macromol. 109 (2018) 483–491, https://doi.org/10.1016/j.ijbiomac.2017.12.100.
[37] A.P. Pawar, K.F. Dubay, J. Zurdo, F. Chiti, M. Vendruscolo, C.M. Dobson, Prediction of "aggregation-prone" and "aggregation-susceptible" regions in proteins associated with neurodegenerative diseases, J. Mol. Biol. 350 (2) (2005) 379–392, https://doi.org/10.1016/j.jmb.2005.04.016.
[38] M. Belli, M. Ramazzotti, F. Chiti, Prediction of amyloid aggregation in vivo, EMBO Rep. 12 (7) (2011) 657–663, https://doi.org/10.1038/embor.2011.116.
[39] J.K. Myers, C. Nick Pace, J. Martin Scholtz, Denaturant m values and heat capacity changes: relation to changes in accessible surface areas of protein unfolding, Protein Sci. 4 (10) (1995) 2138–2148, https://doi.org/10.1002/pro.5560041020.
[40] A. Abedini, D.P. Raleigh, A critical assessment of the role of helical intermediates in amyloid formation by natively unfolded proteins and polypeptides, Protein Eng. Des. Sel. 22 (8) (2009) 453–459 (https://dx.doi.org/10.1093%2Fprotein%2Fgzp036).
[41] J.A. Williamson, J.P. Loria, A.D. Miranker, Helix stabilization precedes aqueous and bilayer-catalyzed fiber formation in islet amyloid polypeptide, J. Mol. Biol. 393 (2) (2009) 383–396 (https://dx.doi.org/10.1016%2Fj.jmb.2009.07.077).
[42] C. Dammers, M. Schwarten, A. Buell, D. Willbold, Pyroglutamate-modified Aβ (3-42) affects aggregation kinetics of Aβ (1-42) by accelerating primary and secondary pathways, Chem. Sci. 8 (7) (2017) 4996–5004, https://doi.org/10.1039/C6SC04797A.
[43] C. Dammers, K. Reiss, L. Gremer, J. Lecher, T. Ziehm, M. Stoldt, M. Schwarten, D. Willbold, Pyroglutamate-modified amyloid-β (3–42) shows α-helical intermediates before amyloid formation, Biophys. J. 112 (8) (2017) 1621–1633, https://doi.org/10.1016/j.bpj.2017.03.007.
[44] N. Taddei, C. Capanni, F. Chiti, M. Stefani, C.M. Dobson, G. Ramponi, Folding and aggregation are selectively influenced by the conformational preferences of the α-helices of muscle acylphosphatase, J. Biol. Chem. 276 (40) (2001) 37149–37154, https://doi.org/10.1074/jbc.m105720200.
[45] Y. Kallberg, M. Gustafsson, B. Persson, J. Thyberg, J. Johansson, Prediction of amyloid fibril-forming proteins, J. Biol. Chem. 276 (16) (2001) 12945–12950 (https://dx.doi.org/10.1186%2F1471-2105-10-S1-S45).
[46] S. Tzotzos, A.J. Doig, Amyloidogenic sequences in native protein structures, Protein Sci. 19 (2) (2010) 327–348, https://doi.org/10.1002/pro.314.
[47] Y.-C. Chen, Impact of a discordant helix on β-amyloid structure, aggregation ability and toxicity, Eur. Biophys. J. 46 (7) (2017) 681–687, https://doi.org/10.1007/s00249-017-1235-5.
[48] C.-J. Lo, C.-C. Wang, H.-B. Huang, C.-F. Chang, M.-S. Shiao, Y.-C. Chen, T.-H. Lin, The Arctic mutation accelerates Aβ aggregation in SDS through reducing the helical propensity of residues 15–25, Amyloid 22 (1) (2015) 8–18, https://doi.org/10.3109/13506129.2014.980943.
[49] B. Ahmad, I. Vigliotta, F. Tatini, S. Campioni, B. Mannini, J. Winkelmann, B. Tiribilli, F. Chiti, The induction of α-helical structure in partially unfolded HypF-N does not affect its aggregation propensity, Protein Eng. Des. Sel. 24 (7) (2011) 553–563, https://doi.org/10.1093/protein/gzr018.